A Quintupled Superstructure of the KHg_2 Type Realized for the New Stannide EuAuSn

Rainer Pöttgen,* Rolf-Dieter Hoffmann, Ralf Müllmann, Bernd D. Mosel and Gunter Kotzyba

Abstract: The title compound was prepared from the elements by reaction in a sealed tantalum tube at 1320 K followed by slow cooling to 970 K. EuAuSn crystallizes with a pronounced subcell of space group *Imma* (KHg_2 type). Additional very weak reflections required a quintupled *b* axis. The superstructure was refined from single-crystal four-circle diffractometer data (*Imm*2, $a = 479.1(1)$ pm, $b = 3833.6(5)$ pm, $c = 820.1(1)$ pm, $Z = 20$, $wR2 = 0.0834$, 3675 F^2 values and 94 variables). Six crystallographically different europium sites occur in the superstructure. Each europium site has an ordered near-neighbour environment of six gold and six tin atoms in the form of two tilted hexagons. Magnetic susceptibility measurements show Curie–Weiss behaviour above 50 K with an experimental magnetic moment of $7.6(1)\mu_B$/Eu, indicating divalent europium. EuAuSn orders antiferromagnetically at about 12 K and undergoes a metamagnetic transition at a critical field of 2.0(2) T. Electrical conductivity measurements show metallic behaviour with a room temperature value of 260 μΩcm. ^{151}Eu and ^{119}Sn Mössbauer spectroscopic experiments are compatible with divalent europium and show complex magnetic hyperfine field splitting at low temperature.

Keywords
conductivity · europium · gold · magnetic properties · superstructures · tin

Introduction

The ternary rare earth (RE)/transition metal (T) intermetallics of the simple composition RETX with X = Ga, In, Si, Ge, or Sn exhibit an unusually large variety of different crystal structures and magnetic properties.[1, 2] Today more than 1000 of these equiatomic compounds are known. They crystallize in more than 30 different structure types.[3] Several of these resemble ordered ternary variants of well-known binary structures.

We have recently synthesized a whole series of new equiatomic EuTX compounds with X = In, Ge, Sn.[4] Most of these intermetallics adopt the KHg_2-type structure[5] with a statistical distribution of the transition metal and X atoms on the mercury position, or crystallize with the TiNiSi-type structure,[6] an ordered ternary version of the KHg_2 type. Characteristic structural motifs of these structure types are chains of transition metal centred trigonal prisms that are formed by the europium and the respective X atoms. With the 33 K ferromagnet EuAuGe (space group *Imm*2)[7, 8] we obtained a newly ordered version of the KHg_2 type. The different ordering in the EuAuGe structure results from a new type of arrangement of the trigonal $[AuGe_2Eu_4]$ prisms. In going to the higher homologue tin, we observed another novel prism arrangement for EuAuSn.

In the present paper we give a full account of the refinements of the subcell and the superstructure of EuAuSn and discuss the crystal chemistry of these structures in the context of a group–subgroup scheme following the Bärnighausen formalism.[9, 10] Additionally, we have determined the magnetic and electrical properties of this new stannide, which we have also investigated by ^{119}Sn and ^{151}Eu Mössbauer spectroscopy.

Experimental Section

Synthesis: Starting materials for the preparation of EuAuSn were ingots of europium (Johnson Matthey), gold wire (Degussa, diameter 1.0 mm) and tin granules (Merck), all with stated purities better than 99.9%. The large europium ingots were cut into smaller pieces in a dry box and kept under argon before reaction. Very careful handling of the europium ingots was necessary in order to minimize the introduction of impurities such as ferromagnetic EuO or EuN, which can irreversibly affect the magnetic measurements. The argon was purified over molecular sieves, titanium sponge (900 K) and an oxisorb catalyst.[11] The elemental components were mixed in the ideal 1:1:1 atomic ratio and sealed in a tantalum tube under an argon pressure of about 800 mbar. The tantalum tube was subsequently sealed in a silica tube to prevent oxidation, and in a first step annealed at 1320 K for two days. The temperature was then lowered by 50 K every other day and finally held at 970 K for three weeks. After the tube had been cooled by radiative heat loss, the silvery product could easily be separated quantitatively from the tantalum tube.

X-ray investigations: A modified Guinier powder pattern[12] of the sample was recorded with $Cu_{K\alpha 1}$ radiation using 5N silicon ($a = 543.07$ pm) as an internal standard. To ensure correct indexing of the diffraction lines, the observed pattern was compared with the calculated one[13] using the positional parameters of the refined structure. The lattice constants were obtained by a least-squares refinement of the Guinier powder data. Single-crystal intensity

[*] Dr. R. Pöttgen, Dr. R.-D. Hoffmann, Dipl.-Chem. G. Kotzyba
Anorganisch-Chemisches Institut, Universität Münster
Wilhelm-Klemm-Strasse 8, 48149 Münster (Germany)
e-mail: pottgen@nwz.uni-muenster.de
Dipl.-Chem. R. Müllmann, Dr. B. D. Mosel
Institut für Physikalische Chemie, Universität Münster
Schlossplatz 4/7, 48149 Münster (Germany)

0947-6539/97/0311-1852 $ 17.50+.50/0

data were collected by use of a four-circle diffractometer (Enraf–Nonius CAD4) with graphite monochromatized $Mo_{K\alpha}$ radiation and a scintillation counter with pulse-height discrimination. Since the superstructure reflections were all very weak, long counting times were chosen in order to achieve a reliable peak/background ratio. The longest total counting time was 240 s per reflection, corresponding to a minimum scan speed for θ of $0.33^\circ\,min^{-1}$. All other relevant data concerning the data collections are listed in Table 1.

Magnetic measurements: The magnetic susceptibilities of polycrystalline pieces were determined with an MPMS SQUID magnetometer (Quantum Design) between 4.2 and 300 K with magnetic flux densities of up to 5.5 T.

Electrical conductivity: The specific resistivities were measured on a small block ($1.3 \times 1.2 \times 1.0\,mm^3$) with a conventional four-probe technique over the temperature range 4.2–300 K. Cooling and heating curves were identical within the error limits, and reproducible for different samples.

Mössbauer spectroscopy: Europium and tin Mössbauer experiments were performed on a polycrystalline sample from the same batch as for the susceptibility measurements. The $^{151}Sm:EuF_3$ and $Ca^{119m}SnO_3$ sources were held at room temperature while the temperature of the absorber was varied between 4.2 and 300 K.

Results and Discussion

Polycrystalline samples of EuAuSn are light grey and stable in air over long periods of time. No decomposition whatsoever was observed after several months. Single crystals have very irregular platelet-like shape and exhibit a metallic lustre.

Lattice constants: The structural similarity of EuAuSn to the KHg_2-type structure was instantly visible on the modified Guinier film.[12] The powder pattern could easily be indexed with a small body-centred orthorhombic cell: $a = 479.20(4)$ pm, $b = 766.85(6)$ pm, $c = 820.26(6)$ pm and $V = 0.30142(5)\,nm^3$.

Table 1. Crystal data and structure refinements for the subcell and the superstructure of EuAuSn.

	Subcell	Superstructure
empirical formula	EuAuSn	
formula weight	$467.62\,g\,mol^{-1}$	
temperature	293(2) K	
wavelength	71.073 pm	
crystal system	orthorhombic	
space group	*Imma* (no. 74)	*Imm*2 (no. 44)
unit cell dimensions	$a = 479.1(1)$ pm	$a = 479.1(1)$ pm
(diffractometer data)	$b = 766.7(1)$ pm	$b = 3833.6(5)$ pm
	$c = 820.1(1)$ pm	$c = 820.1(1)$ pm
	$V = 0.3012\,nm^3$	$V = 1.5063\,nm^3$
formula units per cell	$Z = 4$	$Z = 20$
calculated density	$10.31\,g\,cm^{-3}$	
crystal size	$10 \times 10 \times 20\,\mu m^3$	
scan type	$\bar{\omega}/2\theta$	
absorption correction	from ψ-scan data	
transmission ratio (max/min)	0.997:0.241	
absorption coefficient	$77.03\,mm^{-1}$	
$F(000)$	768	3840
θ range for data collection	2 to 70°	2 to 70°
range in hkl	$\pm 7, \pm 12, \pm 13$	$\pm 7, \pm 61, \pm 13$
total no. reflections	1829	9061
independent reflections	385 ($R_{int} = 0.0662$)	3676 ($R_{int} = 0.0672$)
reflections with $I > 2\sigma(I)$	371 ($R_{sigma} = 0.0360$)	1909 ($R_{sigma} = 0.0724$)
refinement method	full-matrix least-squares on F^2	
data/restraints/parameters	385/0/12	3675/1/94
goodness of fit on F^2	1.351	1.036
final R indices [$I > 2\sigma(I)$]	$R1 = 0.0252$, $wR2 = 0.0604$	$R1 = 0.0294$, $wR2 = 0.0824$
R indices (all data)	$R1 = 0.0266$, $wR2 = 0.0604$	$R1 = 0.0909$, $wR2 = 0.0834$
R (subcell reflections) [a]	–	$675 > 1\sigma(F)$, $R1 = 0.0490$
R (supercell reflections) [a]	–	$1880 > 1\sigma(F)$, $R1 = 0.0462$
R (overall) [a]	–	$2555 > 1\sigma(F)$, $R1 = 0.0470$
extinction coefficient	0.026(1)	0.00092(2)
absolute structure parameter		−0.04(2)
largest diff. peak/hole	$2.483/-2.477\,e\,nm^{-3}$	$4.019/-3.467\,e\,nm^{-3}$

[a] These values were calculated with the program RWERT [14] using the formula $R = \Sigma|F_o - F_c|/\Sigma|F_o|$.

Abstract in German: *Die Titelverbindung wurde durch eine Reaktion der Elemente bei 1320 K in einer geschlossenen Tantalampulle und anschließendes langsames Abkühlen auf 970 K hergestellt. EuAuSn kristallisiert mit einer stark ausgeprägten Unterzelle der Raumgruppe Imma (KHg_2-Typ). Zusätzliche sehr schwache Reflexe bedingten eine Verfünffachung der b-Achse. Die Überstruktur wurde anhand von Einkristalldiffraktometerdaten verfeinert: Imm2; a = 479.1(1) pm; b = 3833.6(5) pm; c = 820.1(1) pm; Z = 20; wR2 = 0.0834; 3675 F^2-Werte und 94 Variable. In der Überstruktur treten sechs kristallographisch unabhängige Europiumatome auf. Jedes Europiumatom hat eine geordnete Umgebung von sechs Gold- und sechs Zinnatomen, welche jeweils in Form zweier geneigter Sechsringe um die Europiumatome angeordnet sind. Magnetische Messungen zeigen Curie–Weiss-Verhalten oberhalb von 50 K mit einem experimentellen magnetischen Moment von 7.6(1) μ_B, was auf zweiwertiges Europium hindeutet. EuAuSn ist ab ca. 12 K antiferromagnetisch und hat einen metamagnetischen Übergang bei einer kritischen Feldstärke von 2.0(2) T. Leitfähigkeitsuntersuchungen zeigten metallisches Verhalten mit 260 $\mu\Omega$cm bei Raumtemperatur. ^{151}Eu- und ^{119}Sn-Mößbauer- spektroskopische Messungen sind in Einklang mit zweiwertigem Europium und lassen bei tiefer Temperatur komplexe magnetische Hyperfeinfeldaufspaltungen erkennen.*

The strongest (121) and two further superstructure reflections (1112 and 1132) were visible on the Guinier pattern only as very weak lines.

Lattice constants of the subcell and the superstructure cell of the single crystal were refined from 25 high-angle reflections on the four-circle diffractometer (see Table 1). The refined data for the subcell reflections of $a = 479.10(1)$ pm, $b = 766.67(1)$ pm, $c = 820.10(1)$ pm and $V = 0.30123(5)\,nm^3$ were in excellent agreement with the lattice constants derived from the Guinier powder data.

Structure determination and refinements: Single crystals of EuAuSn were isolated from the sample by mechanical fragmentation and examined by Buerger precession photographs to establish both symmetry and suitability for an intensity data collection. The photographs (reciprocal layers $hk0$ and $0kl$) clearly showed the quintupled KHg_2-type cell with orthorhombic Laue symmetry *mmm* and the only systematic extinctions found were those for a body-centred lattice. All relevant crystallographic data and experimental details are listed in Table 1. At this point it is noteworthy that the superstructure reflections were observed for all crystals investigated, and also for those of other samples.

The structure of the subcell (KHg_2 type, space group *Imma* with a statistical distribution of gold and tin atoms on the mercury position) was evaluated first. The complete data set was

  0947-6539/97/0311-1853 $ 17.50+.50/0

therefore reduced by eliminating all superstructure reflections and considering only the smaller subcell. The starting atomic parameters were obtained from an automatic interpretation of direct methods with SHELX-86.[15] The subcell structure was subsequently refined with anisotropic displacement parameters for all atoms by means of SHELXL-93.[16] The refined composition for the subcell was $EuAu_{1.04(2)}Sn_{0.96(2)}$. The residuals and atomic coordinates are listed in Tables 1 and 2.

The key to solving the superstructure was to find the ordering for the gold and tin positions along each side of the zigzag chains of the europium atoms (Figure 1). Since the subcell structure of EuAuSn adopts the space group *Imma*, only the subgroups of *Imma* need be considered as possible space groups for the superstructure.[17] In the superstructure both translational and rotational symmetry are lost. Thus, the asymmetric unit of the superstructure is ten times as large as that of the subcell. Such a symmetry reduction of index 10 is only possible in two separate steps: a *translationengleiche* reduction of index 2 (t2) followed by an isomorphic reduction of index 5 (i5) or, equivalently, in the first step an isomorphic reduction of index 5 (i5) followed by a *translationengleiche* reduction of index 2 (t2). The i5 reduction is not a maximal *isomorphic* tranformation of the lowest index and therefore it is not listed in the International Tables.[17] The complete symmetry tree for EuAuSn in going from the aristotype AlB_2 will be discussed later, under the heading Crystal chemistry.

The single-step symmetry reduction of the *translationengleiche* t2 type is already known for EuAuGe.[7, 8] This germanide crystallizes with an ordered version of the KHg_2 type, but without losing translational symmetry. Its space group is *Imm*2, a *translationengleiche* subgroup of index 2 (t2) of *Imma*. From a geometrical point of view, the EuAuGe structure is built up of trigonal $[Eu_4Ge_2]$ prisms centred by gold atoms (Figure 1). Because of the non-centrosymmetricity of the structure and the therefore polar z axis, the germanium atoms of these prisms point only towards the $-z$ direction (Figure 1). We assign to this prism arrangement the notation "– –" for the two prisms along one b translation period.

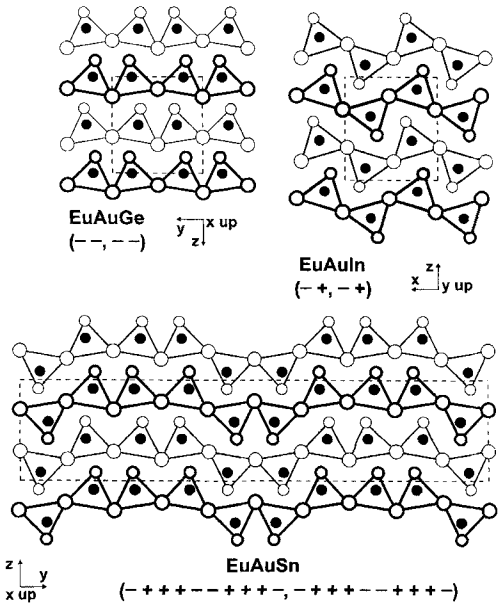

Figure 1. Projections of the crystal structures of EuAuGe, EuAuIn and EuAuSn along the short axis. All atoms lie on mirror planes at $x = 0$ and $x = ½$ (EuAuGe and EuAuSn), indicated by thin and thick lines, respectively. The mirror planes in EuAuIn are at $y = ¼$ and $y = ¾$. The transition metal centred trigonal prisms are outlined. The orientations of the prisms are labelled + if they point in the $+z$ direction and − if they point in the opposite direction.

Table 2. Atomic coordinates and anisotropic displacement parameters (pm^2) for the subcell and the superstructure of EuAuSn. U_{eq} is defined as a third of the trace of the orthogonalized U_{ij} tensor. The anisotropic displacement factor exponent takes the form: $-2\pi^2[(ha^*)^2U_{11} + \ldots + 2hka^*b^*U_{12}]$.

a) Subcell

Atom	*Imma*	x	y	z	U_{11}	U_{22}	U_{33}	U_{23}	U_{eq}
Eu	4*e*	0	¼	0.53971(9)	115(3)	110(3)	100(4)	0	108(2)
M [a]	8*h*	0	0.04399(7)	0.16484(6)	97(2)	213(3)	81(3)	−2(2)	130(2)

b) Superstructure

Atom	*Imm*2	x	y	z	U_{11}	U_{22}	U_{33}	U_{23}	U_{eq}
Eu1	2*b*	½	0	0.7063(3)	97(7)	106(6)	99(10)	0	101(3)
Eu2	4*d*	½	0.80002(3)	0.7069(2)	124(5)	98(4)	87(7)	−10(5)	103(2)
Eu3	4*d*	½	0.60090(3)	0.7097(2)	122(6)	116(4)	82(7)	−6(5)	107(3)
Eu4	2*a*	0	0	0.2910(3)	116(7)	120(7)	107(10)	0	114(4)
Eu5	4*d*	0	0.80039(3)	0.2872(2)	104(5)	99(4)	102(7)	2(5)	101(2)
Eu6	4*d*	0	0.59868(3)	0.2856(2)	97(5)	99(4)	114(7)	8(5)	103(3)
Au1	4*d*	½	0.74332(2)	0.4113(2)	89(3)	151(3)	84(5)	2(5)	108(2)
Au2	4*d*	0	0.93965(2)	0.5825(2)	108(4)	161(4)	93(5)	−2(5)	121(2)
Au3	4*d*	0	0.54372(2)	0.5830(2)	116(4)	147(3)	93(6)	−1(6)	119(2)
Au4	4*d*	½	0.85942(2)	0.4128(2)	97(4)	169(4)	98(6)	−6(4)	121(2)
Au5	4*d*	½	0.65610(2)	0.4119(2)	91(4)	163(3)	91(5)	4(5)	115(2)
Sn1	4*d*	½	0.94022(4)	0.4118(3)	72(7)	209(7)	83(10)	15(8)	121(4)
Sn2	4*d*	½	0.53914(3)	0.4127(3)	75(7)	120(7)	67(9)	4(8)	87(3)
Sn3	4*d*	0	0.73903(4)	0.5811(2)	83(6)	101(5)	71(8)	6(8)	85(3)
Sn4	4*d*	0	0.86033(4)	0.5839(3)	90(7)	125(6)	51(9)	−6(7)	89(3)
Sn5	4*d*	0	0.66074(3)	0.5822(3)	82(6)	104(6)	67(9)	−8(8)	84(3)

[a] M denotes a statistical occupancy of 50% Au and 50% Sn.

0947-6539/97/0311-1854 $ 17.50+.50/0 *Chem. Eur. J.* **1997**, *3*, No. 11

In deducing the superstructure of EuAuSn, three aspects have to be taken into account:

1) It was assumed that the positions of the europium atoms are hardly affected by the ordering of the gold and tin atoms, as was the case for the EuAuGe structure. Thus, each europium position of the superstructure can be precalculated from the subcell parameters.
2) The measurement of the Friedel pairs of all reflections during data collection clearly indicated a non-centrosymmetric structure.
3) The task was to arrange ten gold-centred $[Eu_4Sn_2]$ trigonal prisms in a chain along the y axis of the superstructure cell.

Considering the non-centrosymmetricity, the prism arrangement "$-++++--++++-$" (shown in Figure 1 in the same formalism as for EuAuGe) is the only reasonable one in accordance with the space group *Imm*2 (Figure 2). This ordering scheme was assumed for the calculation of all starting atomic positions from the subcell sites. No damping was necessary during the refinement procedure, which went smoothly to the residuals listed in Table 1.

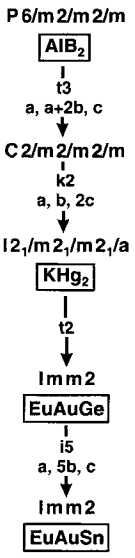

Figure 2. Group–subgroup relationship for EuAuSn starting from the aristotype AlB_2. The indices of the *klassengleiche* (k), the *translationengleiche* (t) and the isomorphic (i) transitions, as well as the unit cell transformations, are given.

As a check for the correct composition, all occupancy parameters were refined in a separate series of least-squares cycles. The occupancy parameters and also the equivalent isotropic displacement parameters gave no indication of mixed occupancy of the gold and tin sites. Within the refinement, only one reflection with $F_o^2 < -2\sigma(F_o^2)$ was treated as unobserved.[16] A final difference Fourier synthesis was flat and revealed no significant residual peaks. The results of the refinement are summarized in Table 1. Atomic coordinates and interatomic distances are listed in Tables 2 and 3. Listings of the observed and calculated structure factors are available.[18] Although the refinement converged to excellent residuals for all reflections, we prefer to calculate separate residuals (Table 1) for the superstructure reflections, since the overall residual is strongly affected by the dominating subcell reflections. The low residuals for the superstructure reflections (assuming a 1σ cutoff) emphasize the high quality of the superstructure refinement.

Crystal chemistry: With EuAuSn we observed a new ordered ternary version of the KHg_2 type. Although such an atomic arrangement is commonly called the $CeCu_2$ type[19] in the literature, we call it the KHg_2 type[5] since KHg_2 is the first compound to have been identified with this structure. EuAuSn belongs to a large family of intermetallic compounds with structures derived from the well-known AlB_2 type. The crystal–chemical relationship in going from the aristotype AlB_2 is shown in a group–subgroup scheme in Figure 2 following a formalism proposed by Bärnighausen.[9, 10] A complete AlB_2 tree with more than 30 different structure types will be published in a forthcoming paper.[20] The complete AlB_2 tree has a hexagonal and an orthorhombic branch. The structure of EuAuSn belongs to the latter. Starting from the aristotype AlB_2, there is a *translationengleiche* symmetry transition of index 3 (t3) from space group *P6/mmm* to space group *Cmmm* followed by a *klassengleiche* transition of index 2 (k2). Thus the KHg_2 type structure in space group *Imma* is reached (Figure 2). At this point it is worthwhile to note that the latter symmetry reduction from the hexagonal to the orthorhombic system allows a tilting of the hexagons surrounding the cation, whereas in all hexagonal structures even the puckered hexagons are *parallel* to each other. Continuing from the KHg_2 structure, we have two possible ways of lowering the symmetry in order to reach the EuAuSn type. One is a *translationengleiche* transition (t2) via the EuAuGe structure (space group *Imm*2) followed by an isomor-

Table 3. Interatomic distances (pm) in EuAuSn. All distances shorter than 475 pm (Eu–Eu, Eu–Au, Eu–Sn) and 410 pm (Au–Au, Au–Sn, Sn–Sn) are listed; standard deviations are all equal or less than 0.2 pm.

Eu1	4 Sn2	329.4	Eu6	1 Au3	322.3	Au5	1 Sn4	276.3
	2 Sn1	332.9		2 Au2	326.7		2 Sn5	277.8
	4 Au2	348.2		2 Sn4	330.8		1 Eu3	323.1
	2 Au3	351.5		1 Sn5	340.2		1 Au1	334.3
	2 Eu6	383.8		1 Sn1	340.9		2 Eu2	337.6
	2 Eu4	416.4		2 Au5	341.4		2 Eu6	341.4
				1 Au4	345.4		1 Eu5	350.0
Eu2	1 Au1	325.6		2 Sn2	346.9			
	1 Au4	331.7		1 Eu1	383.8	Sn1	1 Au3	276.6
	2 Au1	336.3		1 Eu2	393.7		2 Au2	277.4
	2 Au5	337.6		2 Eu3	422.4		1 Au4	309.8
	1 Sn3	341.5					2 Eu3	331.2
	1 Sn5	342.6	Au1	2 Sn3	277.5		1 Eu1	332.9
	2 Sn4	347.8		1 Sn3	279.2		1 Eu6	340.9
	2 Sn3	350.3		1 Eu2	325.6		2 Eu4	346.0
	1 Eu5	390.5		1 Au5	334.3			
	1 Eu6	393.7		2 Eu2	336.3	Sn2	2 Au3	277.9
	2 Eu5	419.4		2 Eu5	340.0		1 Au2	282.8
				1 Eu5	350.8		1 Sn2	300.1
Eu3	1 Au5	323.1					2 Eu1	329.4
	2 Au4	329.1	Au2	2 Sn1	277.4		1 Eu3	339.7
	2 Sn1	331.2		1 Sn2	282.8		1 Eu4	344.6
	1 Sn2	339.7		1 Sn4	304.1		2 Eu6	346.9
	2 Au3	340.9		2 Eu6	326.7			
	1 Sn4	341.0		1 Eu4	332.7	Sn3	2 Au1	277.5
	1 Au2	343.0		1 Eu3	343.0		1 Au1	279.2
	2 Sn5	347.8		2 Eu1	348.2		1 Sn5	300.2
	1 Eu5	383.7					2 Eu5	329.8
	1 Eu4	392.5	Au3	1 Sn1	276.6		1 Eu5	336.8
	2 Eu6	422.4		2 Sn2	277.9		1 Eu2	341.5
				1 Eu6	322.3		2 Eu2	350.3
Eu4	2 Au2	332.7		1 Au3	335.2			
	4 Au3	338.5		2 Eu4	338.5	Sn4	1 Au5	276.3
	2 Sn2	344.6		2 Eu3	340.9		2 Au4	277.7
	4 Sn1	346.0		1 Eu1	351.5		1 Au2	304.1
	2 Eu3	392.5					2 Eu6	330.8
	2 Eu1	416.4	Au4	2 Sn4	277.7		1 Eu5	334.7
				1 Sn5	281.9		1 Eu3	341.0
Eu5	2 Sn5	328.4		1 Sn1	309.8		2 Eu2	347.8
	2 Sn3	329.8		2 Eu3	329.1			
	1 Sn4	334.7		1 Eu2	331.7	Sn5	2 Au5	277.8
	1 Sn3	336.8		2 Eu5	345.3		1 Au4	281.9
	2 Au1	340.0		1 Eu6	345.4		1 Sn3	300.2
	2 Au4	345.3					2 Eu5	328.4
	1 Au5	350.0					1 Eu6	340.2
	1 Au1	350.8					1 Eu2	342.6
	1 Eu3	383.7					2 Eu3	347.8
	1 Eu2	390.5						
	2 Eu2	419.4						

  0947-6539/97/0311-1855 $ 17.50+.50/0

phic transition of index 5 (i5). On the other hand this symmetry reduction can be attained by an isomorphic transition of index 5 (i5) to space group *Imma* followed by a *translationengleiche* transition (t2). We have considered the first way, since the EuAuGe structure in space group *Imm*2 is already known to exist (Figure 2).

From a geometric point of view, the structure of EuAuSn can be built up from trigonal prisms. The europium atoms form zigzag chains running along the y axis at two different heights ($x = 0$ and $x = {}^1/_2$). Together with the tin atoms, the zigzag chains form trigonal prisms, which are centred by the gold atoms. Three-fifths of these trigonal prisms point towards the $+z$ direction while the other two-fifths point towards the $-z$ direction. This is the direct reason for the non-centrosymmetricity of the structure. For a better comparison, the structure of two other ordered ternary variants of KHg_2 are also presented in Figure 1. In the well-known centrosymmetric TiNiSi-type structure of EuAuIn, the trigonal $[AuEu_4In_2]$ prisms are alternately arranged in the $+z$ and $-z$ direction, while the $[AuEu_4Ge_2]$ prisms in EuAuGe point exclusively in the $-z$ direction. Considering this geometrical view, the different ordering variants are clearly distinguishable.

For a closer look at the EuAuSn structure, it is interesting to compare the individual coordination polyhedra. All six crystallographically different europium atoms have coordination number (CN) 16, with six gold, six tin and four europium atoms in their coordination shell (Figure 3) with the gold and tin atoms forming different distorted and tilted Au_3Sn_3 hexagons. Whereas the polyhedra have an almost identical europium coordination, there are large differences in the coordination by the gold and tin atoms. The most remarkable feature of the coordination polyhedra is the tilting of the different Au_3Sn_3 hexagons, which directly results from the symmetry reduction from the hexagonal to the orthorhombic crystal system. This tilting strongly influences the europium coordination.

In hexagonal EuCuGe with the AlB_2-type structure,[4] each europium atom has six europium neighbours within the basal hexagonal plane (at the same distance) and two further europium atoms perpendicular to it. The copper and germanium atoms form a sandwich-like coordination of two Cu_3Ge_3 hexagons around each europium atom (Figure 3). Because of the strong tilting of the hexagons in EuAuSn, two of the six europium atoms from the basal plane are now at shorter distances from the central europium atom, while the four other europium atoms have moved away. This is a direct consequence of the Eu–Eu zigzag chains (Figures 1 and 3), as can be seen by comparison with the straight lines in the highly symmetric AlB_2-type structure of EuCuGe. The six europium polyhedra (Figure 3) can be divided into three groups with similar coordination.

There are three different arrangements of the Au_3Sn_3 hexagons present. Whereas the gold and tin atoms within the tilted hexagons are directly superimposed for Eu1, Eu2, Eu4 and Eu5, the hexagons are rotated by about 60° for Eu3 and Eu6. This results in weak Au–Au and stronger Sn–Sn interactions between neighbouring gold and tin atoms for the Eu1, Eu2, Eu4 and Eu5 polyhedra, whereas there are only Au–Sn interactions between the hexagons for Eu3 and Eu6. The tilting of the hexagons consequently leads to the formation of chains of different Au_2Sn_2 squares (Figure 3).

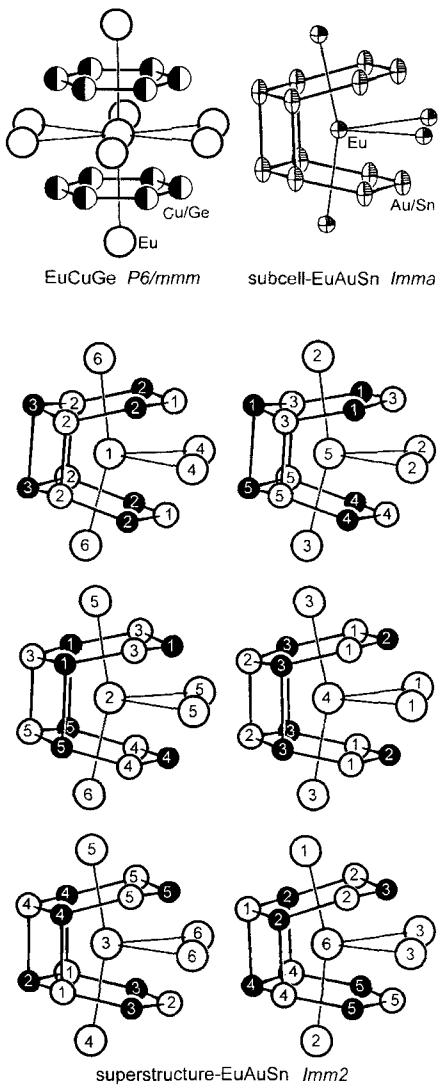

Figure 3. Coordination polyhedra of the europium atoms in the structures of EuCuGe (AlB_2 type) and EuAuSn. All the neighbours listed in Table 3 are drawn. The anisotropic displacement parameters of the subcell polyhedron are drawn with a 95% probability limit.

The Au–Sn intralayer distances within the different Au_3Sn_3 hexagons vary from 276.3 to 282.8 pm with an average value of 278.2 pm. This average Au–Sn distance is only slightly larger than the sum of Pauling's single bond radii of 273.5 pm for gold and tin,[21] indicating essentially covalent bonding within these hexagons. These distances compare well with the average Au–Sn distance of 275.3 pm in NaAuSn, which has a TiNiSi-type structure.[22, 23] The interlayer Au–Sn distances of 304.1 and 309.8 pm in the polyhedra around Eu3 and Eu6 are much longer.

The different Au–Au distances between the hexagons range from 334.3 to 335.2 pm, and the Sn–Sn distances from 300.1 to 300.2 pm. The Sn–Sn interactions may certainly be considered to be bonding in comparison with β-tin, where each tin atom has two neighbours at 302 pm and two further neighbours at 318 pm forming a flattened tetrahedron.[24] The formation of these Sn–Sn bonds may be one reason for the formation of the superstructure and for the stability of this compound. The Au–Au interactions are only weak in comparison with the corre-

0947-6539/97/0311-1856 $ 17.50+.50/0 *Chem. Eur. J.* **1997**, *3*, No. 11

sponding Sn–Sn interactions. The interlayer Au–Au distances of 334.3 and 335.2 pm are significantly longer than in *fcc* gold,[24] where each gold atom has twelve neighbours at 288.4 pm. The interlayer Au–Au distances of 316.0 pm in EuAuGe[7, 8] and of 327.9 pm in Er_2Au_2Sn[25] may also be considered to be weak interactions. All these distances compare well with those in molecular compounds such as $[\{Au(i\mathrm{PrO})_2PS_2\}_2]$,[26] $[i\mathrm{PrNH_2AuC{\equiv}CC_6H_5}]$[27] or $[Au^{III}(DMG)_2Au^{I}Cl_2]$,[28] where such secondary Au–Au bonds (291.4 up to 327 pm) are sufficiently strong to cause dimerization in solution and polymerization in the solid state. Similar weak Au–Au interactions were also observed in Au_2P_3 and $Au_7P_{10}I$.[29]

Similarly, different arrangements of the hexagons are also present in the hexagonal structures of ScAuSi and YAuSi,[30] but the puckered hexagons in these structures are parallel to each other. Whereas the yttrium silicide crystallizes with the LiGaGe-type structure in space group $P6_3mc$ with staggered Au_3Si_3 hexagons, ScAuSi adopts its own structure type (space group $P\bar{6}m2$) with an eclipsed arrangement of the Au_3Si_3 hexagons. This results in weak Au–Au (294 pm) and Si–Si (276 pm) interactions between the hexagons.

Chemical bonding in EuAuSn may to a first approximation be described by the concept of a polyanionic network. The europium atoms are by far the most electropositive component of EuAuSn, and they will largely have transferred their two valence electrons to the three-dimensional [AuSn] network. The divalent character of the europium atoms was determined by magnetic susceptibility and ^{151}Eu Mössbauer spectroscopic measurements (see below). The formula of our compound may then be written as $Eu^{2+}[AuSn]^{2-}$, but, because of the complex atom distribution within the three-dimensional polyanion, a simple assignment of oxidation numbers is clearly not possible.

A more detailed view of chemical bonding in KHg_2- and TiNiSi-type intermetallic compounds based on extended Hückel calculations was given in a very recent paper by Nuspl et al.[23] These authors investigated the crystal and electronic structures of the isotypic TiNiSi-type compounds CaPdIn, CaPdSn, CaPdSb and CaAgSb. In these four palladium intermetallics the T_2X_2 rectangles within the [TX] polyanions are all tilted in order to maximize the distance (i.e. minimize the repulsion) between the more electronegative atoms. We observed this independently, from the structure refinements of a whole series of such intermetallic compounds with europium as the electropositive component.[4]

However, for the recently reported germanides EuAuGe[7, 8] and NaAuGe[31] as well as for EuAuSn, we observe new arrangements of these rectangles. In these three compounds the tilted hexagons are stacked on each other; this results in weak Au–Au, Ge–Ge and Sn–Sn interactions within some of these rectangles. The different arrangements of the T_2X_2 rectangles in EuAuSn are outlined in Figure 3. Theoretical studies of the electronic structures of EuAuGe and EuAuSn are now in progress.

In Figure 3 we also present the coordination polyhedron of the europium atom in the subcell refinement, drawn with anisotropic displacement parameters. The larger U_{22} parameter for the 8*h* position of the subcell refinement (Table 2) is a direct indication of an ordering between the gold and tin atoms. The clearest indication of the superstructure, however, was given by the additional reflections on the Buerger photographs. Yet in several other disordered KHg_2-type compounds[4, 32–34] where the U_{22} parameters are also about three times as large as U_{11} and U_{33}, no superstructure reflections occur. We interpret these larger U_{22} values as an indication of a large degree of short range order within these compounds.

At this point it is important to ask whether or not other compounds may be ordered, especially those with large differences in scattering factors between the transition metal and the main-group element that are described as having a statistical distribution (disordered KHg_2-type). Only detailed investigations of single crystals can clarify this question.

We have recently investigated the ternary compounds EuZnGa,[34] EuAgGa, EuAuGa,[35] EuZnIn,[4] EuAgIn,[36] EuAgGe,[33] EuCuSn and EuAgSn[32] by X-ray diffraction of single crystals, first by Buerger precession photographs and later by refining their structures from four-circle diffractometer data. However, none of these compounds, even EuAuGa, with large differences in the scattering factors between gold and gallium, showed any superstructure reflections indicating an ordering between the transition metal and main group element. These results may be attributable to a deviation from the correct 1:1:1 composition indicating homogeneity ranges; however, the compositions refined from the single-crystal X-ray data were all very close to the ideal compositions EuTX. High-resolution electron microscopy may be helpful for studying the short-range order of this interesting class of compounds.

In summary, we have observed a new quintupled superstructure of the KHg_2 type structure which elegantly extends the rich crystal chemistry of AlB_2-related intermetallic compounds.

Magnetic and electrical properties: The temperature dependence of the inverse susceptibility of EuAuSn is presented in Figure 4.

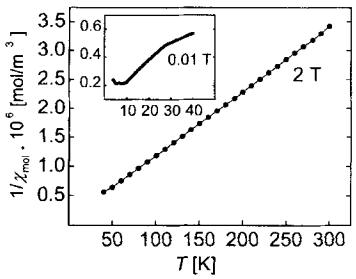

Figure 4. Temperature dependence of the inverse magnetic susceptibility of EuAuSn measured at a magnetic flux density of 2 T. The inset shows the low-temperature data obtained at 0.01 T.

EuAuSn shows Curie–Weiss behaviour above 50 K. The straight line indicates the absence of a possible EuO impurity ($T_C = 70$ K). The magnetic moment of $\mu_{exp} = 7.6(1)\mu_B$ deduced from the Curie–Weiss graph is in good agreement with the theoretical value of $\mu_{eff} = 7.94\mu_B$ for the free Eu^{2+} ion. The paramagnetic Curie temperature (Weiss constant) of $-8(1)$ K was obtained by extrapolation of the linear $1/\chi$ versus T plot to $1/\chi = 0$. EuAuSn orders antiferromagnetically at 8.5(5) K at small magnetic flux densities, as is evident from the inset of Figure 4. A second minimum is apparent in this curve at

  0947-6539/97/0311-1857 $ 17.50+.50/0

5.5(5) K, most probably due to a different antiferromagnetic spin alignment. Magnetic ordering has already been detected at 12 K by the Mössbauer experiments, as discussed below. The dependence of magnetization on external flux density is shown in Figure 5. In this plot we observe a straight line up to a flux

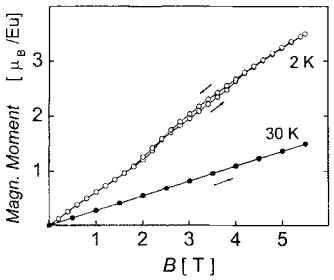

Figure 5. Magnetization vs. external magnetic flux density of EuAuSn at 2 and 30 K.

density of 2.0(2) T, as can be expected for an antiferromagnet. The magnetization curve shows a slight curvature above 2 T, indicating a metamagnetic transition (antiferromagnetic to ferromagnetic spin alignment). The magnetic moment at the highest obtainable flux density of 5.5 T amounts to $3.5(1)\,\mu_B$/Eu at 2 K, much smaller than the maximum saturation moment of $7.0\,\mu_B$ for divalent europium. In view of the six crystallographically different europium positions in the superstructure, one can easily understand that the nature of magnetic ordering in EuAuSn is very complex.

The specific resistivity (ρ) of EuAuSn (Figure 6) decreases with decreasing temperature, as is usual for metallic conductors. The room-temperature value of the specific resistivity of 260 μΩcm indicates quite good metallic conductivity for this ternary stannide.

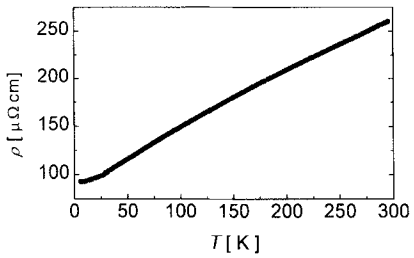

Figure 6. Temperature dependence of the specific resistivity of EuAuSn.

^{119}Sn and ^{151}Eu Mössbauer spectroscopy: ^{151}Eu Mössbauer spectra at 78, 9.2 and 4.2 K are presented in Figure 7, together with theoretical transmission integral fits including static magnetic hyperfine splitting. The fitting parameters for these and some additional measurements are listed in Table 4. Above the magnetic ordering temperature of 12 ± 1 K (as determined by ^{151}Eu Mössbauer spectroscopy; compare with the magnetic data above) a single line is detected in the Eu^{II} region with an isomer shift $\delta = -11.0$ mm s^{-1} at room temperature and with vanishing electric field gradient. In the Eu^{III} region an impurity component can be seen at $\delta = 1.3$ mm s^{-1}, which is included as a simple Lorentzian in all fits, but not reported in the table. At 4 K the area of the impurity is about 7% of the total area.

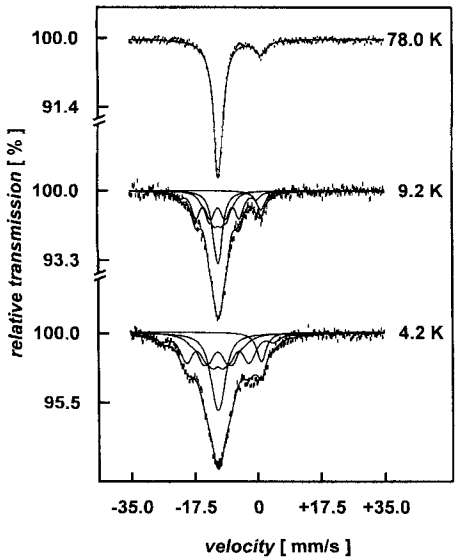

Figure 7. ^{151}Eu Mössbauer spectra of EuAuSn containing a small amount of an Eu^{III} impurity.

Table 4. Fitting parameters of ^{151}Eu Mössbauer measurements on EuAuSn. Numbers in parentheses represent the statistical errors in the last digit. Parameters without parentheses were kept fixed. Linewidth parameters and isomer shifts of the different components were coupled.

T/K	δ/mm s^{-1}	Γ/mm s^{-1}	$\lvert B_1\rvert$/T	$\lvert B_2\rvert$/T	$\lvert B_3\rvert$/T
300	−11.02(3)	2.3	–	–	–
78	−10.86(4)	2.3(1)	–	–	–
14.7	−10.94(6)	2.2(2)	–	–	–
13.8	−10.80(5)	2.3(1)	–	–	–
11	−10.73(7)	2.3	7.6(8)	4.3(7)	–
9.2	−10.68(9)	2.3	14.8(6)	6.1(7)	1.4(5)
4.2	−10.88(9)	3.5(4)	21.4(6)	10.3(9)	2.2(6)

Below the ordering temperature the Eu^{II} spectrum is symmetric, indicating that the quadrupole interactions are negligible. The magnetically split spectrum can be fitted by three hyperfine components with ratios fixed at 4:3:3. This ratio agrees reasonably well with crystallographic information, indicating that the six different Eu sites can be grouped into three pairs (see Figure 3) of very similar coordination. At 4.2 K the internal fields of the three components are very different, amounting to 21.4, 10.3 and 2.2 T. At this temperature the enhanced linewidths of the fit indicate that the grouping into three components is only an approximation. The six crystallographically different europium sites certainly cause a very complex hyperfine field splitting at low temperature.

The ^{119}Sn Mössbauer spectra are shown in Figure 8, together with the fits. The fitting parameters are given in Table 5. Above the magnetic ordering temperature of europium, the spectrum is fitted well by one component with an isomer shift $\delta = 1.93$ mm s^{-1} at room temperature and a quadrupole splitting $\Delta E_Q = 0.77$ mm s^{-1}. In this signal a tin impurity must be included, corresponding to the Eu impurity mentioned above. In a previous Mössbauer study on EuZnSn[37] with only a single tin site, tin was subjected to a large transferred magnetic hyperfine field of 12.8 T at 4.2 K. The magnetically split spectrum was then well separated from the signal of the impurity, which was

0947-6539/97/0311-1858 $ 17.50+.50/0 Chem. Eur. J. 1997, 3, No. 11

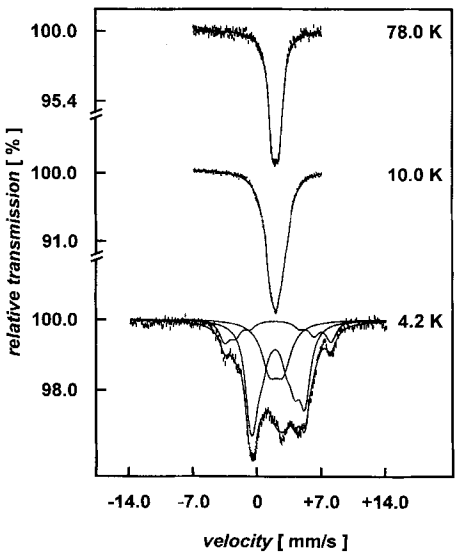

Figure 8. ^{119}Sn Mössbauer spectra of EuAuSn showing transferred magnetic hyperfine fields below the magnetic ordering temperature of europium. The small magnetic hyperfine splitting of the central component is simulated by line broadening.

Table 5. Fitting parameters of ^{119}Sn Mössbauer measurements on EuAuSn. Linewidth parameters, isomer shifts and electrical field gradients of the different components are identical except that the small hyperfine splitting of the most prominent peak in the spectrum in Figure 8 is simulated by Lorentzian line broadening $\Delta_3 = 2.1(4)$ mm s^{-1} at 4.2 K.

T/K	δ/mm s^{-1}	Γ/mm s^{-1}	ΔE_Q/mm s^{-1}	$\lvert B_1\rvert$/T	$\lvert B_2\rvert$/T
300	1.93(1)	0.98(4)	0.77(3)	–	–
78	1.98(2)	1.04(6)	0.76(4)	–	–
15	1.99(1)	1.03(5)	0.77(3)	–	–
10	1.97(1)	1.52(6)	−0.38	0.7(2)	–
4.2	1.98	1.4(1)	−0.38	8.3(2)	4.2(1)

located near 2.1 mm s^{-1} and was therefore hidden when hyperfine fields were smaller or totally absent.

In EuAuSn magnetic hyperfine fields are also transferred to the various tin sites below the ordering temperature of europium. As in the europium spectrum, three subspectra were used to fit the experimental data with intensities in the ratio 1:3.5:1 at 4.2 K. Two magnetic flux densities of $|B_1| = 8.3$ and $|B_2| = 4.2$ T are well separated at 4.2 K. Their directions are both perpendicular to that of the electrical field gradient principal axis, which results in a change of ΔE_Q by a factor of $-{}^1/_2$ and produces the correct asymmetry of the signal. The third component of the magnetic hyperfine spectrum represents the tin sites with a small transferred hyperfine magnetic field. This component is simulated by a simple Lorentzian curve and also includes the presumed impurity near 2.1 mm s^{-1}.

Acknowledgments: We thank Professor H. Eckert and Professor W. Jeitschko for their interest and steady support of this work. We are also grateful to Professor H. Bärnighausen for fruitful discussions concerning the group–subgroup schemes. Special thanks go to Dipl.-Ing. U. Rodewald for the collection of intensity data, to W. Röthenbach for taking the Guinier powder patterns and to N. Rollbühler and Dr. R. K. Kremer for the electrical conductivity measurement. This work was supported by the Deutsche Forschungsgemeinschaft (Po573/1) and the Fonds der Chemischen Industrie.

Received: April 8, 1997 [F659]

[1] P. Villars, L. D. Calvert, *Pearson's Handbook of Crystallographic Data for Intermetallic Phases*, American Society for Metals, Metals Park, OH 44073, USA, **1991**.
[2] A. Szytuła, J. Leciejewicz, *Handbook of Crystal Structures and Magnetic Properties of Rare Earth Intermetallics*, CRC Press, Boca Raton, Florida, **1994**.
[3] F.Merlo, M. L. Fornasini, *J. Alloys Compd.* **1995**, *219*, 63.
[4] R. Pöttgen, *Z. Kristallogr.* **1996**, *211*, 884 and references therein.
[5] E. J. Duwell, N. C. Baenziger, *Acta Crystallogr.* **1955**, *8*, 705.
[6] C. B. Shoemaker, D. P. Shoemaker, *Acta Crystallogr.* **1965**, *18*, 900.
[7] R. Pöttgen, *J. Mater. Chem.* **1995**, *5*, 505.
[8] R. Müllmann, B. D. Mosel, H. Eckert, R. Pöttgen, R. K. Kremer, *Hyp. Int.* **1997**, *108*, 389.
[9] H. Bärnighausen, *Commun. Math. Chem.* **1980**, *9*, 139.
[10] H. Bärnighausen, U. Müller, *Symmetriebeziehungen zwischen den Raumgruppen als Hilfsmittel zur straffen Darstellung von Strukturzusammenhängen in der Kristallchemie*, University of Karlsruhe and University Gh. Kassel, Germany, **1996**.
[11] H. L. Krauss, H. Stach, *Z. Anorg. Allg. Chem.* **1969**, *366*, 34.
[12] A. Simon, *J. Appl. Crystallogr.* **1971**, *4*, 138.
[13] K. Yvon, W. Jeitschko, E. Parthé, *J. Appl. Crystallogr.* **1977**, *10*, 73.
[14] R.-D. Hoffmann, RWERT, Program for Calculation of *R* values for Specific Classes of Reflections, University of Münster, Germany, **1996**.
[15] G. M. Sheldrick, SHELX-86, Program for the Determination of Crystal Structures, University of Göttingen, Germany, 1993.
[16] G. M. Sheldrick, SHELXL-93, Program for Crystal Structure Refinement, University of Göttingen, Germany, **1993**.
[17] *International Tables for Crystallography* (ed. Th. Hahn), 4th ed., Kluwer Academic Publishers, Dordrecht, **1996**.
[18] Further details of the crystal structure investigations may be obtained from the Fachinformationszentrum Karlsruhe, 76344 Eggenstein-Leopoldshafen (Germany) on quoting the depository number CSD-406808.
[19] A. C. Larson, D. T. Cromer, *Acta Crystallogr.* **1961**, *14*, 73.
[20] R. Pöttgen, R.-D. Hoffmann, unpublished results.
[21] L. Pauling, *The Nature of the Chemical Bond and the Structure of Molecules and Crystals*, Cornell University Press, Ithaca, NY, **1960**.
[22] G. Wrobel, H.-U. Schuster, *Z. Anorg. Allg. Chem.* **1977**, *432*, 95.
[23] G. Nuspl, K. Polborn, J. Evers, G. A. Landrum, R. Hoffmann, *Inorg. Chem.* **1996**, *35*, 6922.
[24] J. Donohue, *The Structures of the Elements*, Wiley, New York, **1974**.
[25] R. Pöttgen, *Z. Naturforsch. Teil B* **1994**, *49*, 1309.
[26] S. L. Lawton, W. J. Rohrbaugh, G. T. Kokotailo, *Inorg. Chem.* **1972**, *11*, 2227.
[27] P. W. R. Corfield, H. M. M. Shearer, *Acta Crystallogr.* **1967**, *23*, 156.
[28] R. E. Rundle, *J. Am. Chem. Soc.* **1954**, *76*, 3101.
[29] W. Jeitschko, M. H. Möller, *Acta Crystallogr. Sect.B* **1979**, *35*, 573.
[30] M. L. Fornasini, A. Iandelli, M. Pani, *J. Alloys Compd.* **1992**, *187*, 243.
[31] U. Zachwieja, *Z. Anorg. Allg. Chem.* **1996**, *622*, 1173.
[32] R. Pöttgen, *J. Alloys Compd.* **1996**, *243*, L1.
[33] R. Pöttgen, *Z. Naturforsch. Teil B* **1995**, *50*, 1071.
[34] J. Grin, R. Pöttgen, G. Kotzyba, unpublished results.
[35] R. Pöttgen, Yu. Grin, *Z. Kristallogr.* **1996**, *Suppl. 11*, 93.
[36] R. Pöttgen, unpublished results.
[37] U. Ernet, R. Müllmann, B. D. Mosel, H. Eckert, R. Pöttgen, G. Kotzyba, *J. Mater. Chem.* **1997**, *7*, 255.

  0947-6539/97/0311-1859 $ 17.50+.50/0